Available online at www.sciencedirect.com

ScienceDirect

Procedia CIRP 87 (2020) 245–250

www.elsevier.com/locate/procedia

5th CIRP CSI 2020

Influence of lubrication condition on the surface integrity induced during drag finishing

I.Malkorra[a,b] *, F. Salvatore[b], J. Rech[b], P.Arrazola[c], J. Tardelli[a], A.Mathis[d]

[a]IRT-M2P, 4 Rue Augustin Fresnel, 57070 Metz, France
[b] University of Lyon, ENISE, LTDS CNRS UMR 5513, 58 Rue Jean Parot, 42000 Saint-Etienne, France
[c]Faculty of Engineering, Loramendi 4, Mondragon University, 2500 Arrasate, Spain
[d]Naval Group, CESMAN, Technocampus Ocean, 5 rue de l'Halbrane, 44340 Bouguenais, France

* Corresponding author. Tel.: +33 06 12 06 97 33. *E-mail address:* irati.malkorra@enise.fr

Abstract

Tribofinishing is one of the most popular polishing process in industry. The action of small abrasive media around parts enables to reduce significantly surface roughness and at the same time, to induce compressive residual stresses in the external surface layer. However, few scientific investigations have been made about this process. Whereas most of the previous works were focused on the effect of abrasive grains, the influence of lubrication and especially the filtering of the lubricant on the surface integrity have never been investigated before. This paper aims to study the influence of the presence of debris coming from the part and the media in the polishing process. For that purpose, rough surface parts (*Ra*~15 µm) have been tribofinished without and with lubrication filtering. Roughness parameters (*Ra*, *RSm* and *Rsk*), the offset between surface profiles and residual stresses have been compared. It is revealed that the lack of filtering leads to the presence of debris coming from the part and the media. This modifies tremendously the action of the media and prevent the surface from being polished properly. The reduction of roughness is saturated and the material is excessively deformed as a consequence of debris incrustations in the surface.

Keywords: Drag finishing; Surface modification; Lubrication.

1. Introduction

Tribofinishing is a superfinishing process that enables surface roughness improvement due to the flow of abrasive media around the workpiece. It also enhances its functional performance like induces compressive residual stresses as well as high surface hardness [1]. Different processes exist depending on the kinematics of the systems: vibratory finishing, rotary barrel, drag finishing, stream finishing, etc. Regardless of the kinematics, all systems consists of a bowl charged with loose abrasive media, a liquid compound and workpieces (loose or fixed) [2–4].

Drag finishing process is one of the most popular techniques after vibratory finishing. The workpiece, fixed to a spindle, is dragged through abrasive media and liquid compound while it rotates around its axe to have a uniform surface improvement. Higher velocities than in the vibratory finishing process can be applied and various parts can be treated at the same time.

Hashimoto described the abrasive process on a microscopic scale in [5], which depends on the velocity of the abrasive, the impact angle and its rotation. Yabuki has also identified various contact types analysing experimentally measured force signals in vibratory finishing [6]. Relative velocities between part and media flux result in material removal and plastic deformation. The proportion of abrasion and deformation will be defined by process parameters like as media shape and dimensions, velocity, etc. [3].

Most of the scientific papers were focused on vibratory finishing, in the modelling of media behaviour, the effect of

2212-8271
10.1016/j.procir.2020.02.087

kinetic energy and the effect of the type of media in *Ra* reduction.

Hashimoto [7] proposed a model that predicts the dynamic motion of the abrasive media during tribofinishing. In [8] they completed the previous work by analysing media-part interactions (contact forces, sliding velocity, etc.) with a discrete element model. This data has been correlated with a wear law to create a material removal model for vibratory finishing [9].

Song et al. [10] measured contact forces in vibratory finishing, showing that higher vibration frequencies (f=15–25 Hz) increase number and intensity of contacts. Ciampini has also characterized impact forces using a force sensor [11] and an Almen system [12]. However, none of them analysed the effect of the amplitude (A=0.7-1.4 mm), which plays a very important role in determining media velocity as Pandiyan et al. [13] showed. They observed that higher velocities result in a faster *Ra* reduction. New generation high frequency vibratory finishers have been developed to increase efficiency: at f=40 Hz, process time is reduced by 40% compared with conventional machines of f=25 Hz [14].

Comparative studies about the use of distinct media have also been published. Size and weight of media will determine impact forces as Song et al. measured [10]. Heavier media will create higher impact forces. Since abrasive wear increases with higher impact forces (Archard's law) [15], tribofinishing process will be more efficient with heavier media. The shape of media influences on the mechanisms of ploughing or cutting in part surface. Uhlmann [16] reported that abrasion and micro-cutting is assumed for spherical media, and cutting for triangular media.

However, tribofinishing processes involve more parameters that have received little research attention: the liquid compound. The compound plays an important role in the final part finish, Mediratta [14] showed that with increasing liquid compound (water), better surface finish (*Ra*) is obtained. Wang et al. [17] tested different lubrication conditions (dry, water-wet and detergent) and showed that the efficiency of the process decreases with water-wet or detergent. As Yabuki et al. [6] measured, water-wet condition creates lower dynamic coefficients of friction than dry condition. Lower friction will lead to less plastic surface deformation per impact, but lower *Ra* will be created.

Nevertheless, none publication has investigated the effect of the lubrication filtration. During tribofinishing processes, a debris is created from the abrasion of the part and the media. This must be evacuated by means of circulating and filtering liquid compound. Otherwise, the debris will remain between media and part surface, modifying the material removal and deformation rate. This will be unfavourable when polishing additive manufactured parts, as the debris will enter into surface defects as cavities, roughness profile valleys, etc.

The present paper shows the importance of lubrication condition during tribofinishing processes. It highlights that the presence of debris can deteriorate the surface integrity of the part. Rough surface parts (*Ra*~15 µm) have been tribofinished with two lubrication conditions (section 3.1). Roughness parameters (*Ra*, *RSm* and *Rsk*), the offset between surface profiles and residual stresses have been compared.

2. Working methodology

2.1. Material properties

A ferritic-pearlitic steel (C45) has been selected for the study. The chemical composition is shown in Table 1. The material presents a hardness of 200 HV. The mechanical properties of the material have been extracted from the literature [18]: ρ=7764 kg/m^3 (T=20°C), E=210·10^3 MPa, υ=0.3.

Table 1. Chemical composition of C45:

C	Si	Mn	S	P	Ni	Cr	Mo	Cu	Al
0.45	0.33	0.78	0.025	0.014	0.09	0.12	0.02	0.11	0.007

2.2. Sample geometry and surface characteristics

Four samples have been manufactured of a medium carbon steel (C45), see Section 2.1. A periodic surface of *Ra*~12 µm has been created by milling in a 60 mm long and a diameter of 20 mm cylinders. Fig.1(a) explains the milling process. The milling tool used was MC232-06.0W2B-WJ30ED and the cutting conditions were: V_c=200 [m/min]; the feed per tooth f_z =0.05 [mm], axial depth of cut a_p=0.07 [mm]; radial depth of cut a_e=0.07 [mm] and lubricant emulsion was used.

The manufactured surface (Fig.1, (c)) represents an additive manufactured surface (a high *Ra*). Since it is periodical and uniform, facilitates the analysis and comparison of tribofinished surfaces. The surface exhibits next roughness parameters: *Ra*~12 µm, *RSm*~100µm and *Rsk*~1.

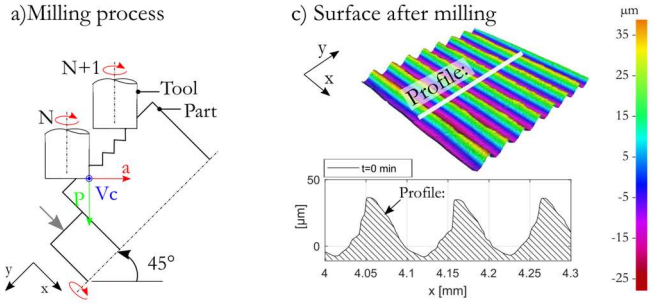

Fig.1. (a) Milling process and (b) the surface after milling.

2.3. Experimental equipment

An original experimental set-up was designed to study the surface evolution under media impacts during tribofinishing. A drag finishing machine of the provider ABC Swiss Tech (Fig.2, (a)) has been modified to drag the sample through the media and compound solution with a circumferential path (Fig.2, (b)). The same kinematic of drag finishing machines has been maintained, but in this case, the part does not rotate around its axe. This movement permits having always the same sample surface, referred to as "frontal zone", treated with a constant and normal flow of media (Fig.2, (c)). The present experimental method has been patented by Grange et al. [19].

Salvatore et al. [20] have verified the efficiency of this method. They showed that surface is exposed to different media trajectories depending on its position. For example, the "frontal

zone" is impacted with high normal velocity and low tangential speed. In this case, the deformation and hardening of the material happens. Whereas in the "lateral zone" the impacts are combined with high tangential velocity. Scratching phenomena is present in this zone (Fig.2, (c)).

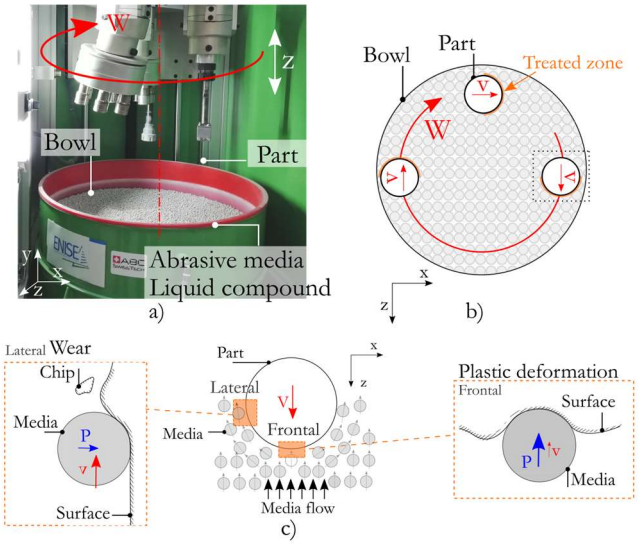

Fig.2. a) The experimental set-up, b) imparted motion to the part in 2D, c) media flow and wear and plastic deformation mechanisms.

2.4. Surface characterization method

Surface topography

This paper focuses on the surface topography modification in the frontal zone, where mostly plastic deformation happens. Cylindrical samples with a rough and periodical surface have been manufactured (see section 3) to represent additive manufactured (SLM) rough surfaces. Those surfaces have been characterised with a confocal microscope "ALICONA Infinite Focus" before and during the tribofinishing process at t=0, 5, 20, 60, 210 min (330 min in the case of S-1). The respective magnification, the vertical and lateral resolutions used have been 20x, 0.1 µm and 2.5 µm. Surfaces of 0.8 x 5 mm have been measured. Roughness parameters such as *Ra*, *RSm* and *Rsk* have been extracted from 4 mm long 2D profiles (perpendicular to roughness direction, see the profile line in Fig.1,(c)). No Gaussian filters have been applied. *Ra* reveals the average profile height, *RSm* describes the distance between irregularities and *RSk* shows if the surface is made of peaks (*RSk*>0) or valleys (*RSk*<0) (Fig.3, (a)).

Offset between surface profiles

A reference (scratch) has been made on each sample (Fig.3, (b),(c)), which would not be modified during tribofinishing. The surfaces (including the references) have been measured with ALICONA before and after polishing the sample (Fig.3, (c)). By means of superposing surface profile lines, the offset (Δ) between them will reveal the quantity of material removal or deformation happened.

The height of the initial profile is called as R_t, (distance between peaks and valleys in vertical direction). If the final profile line is below the initial one (so $\Delta > R_t$), it may say that a significant material removal happened. However, sometimes media action is not able to remove initial surface profile (when $\Delta < R_t$).

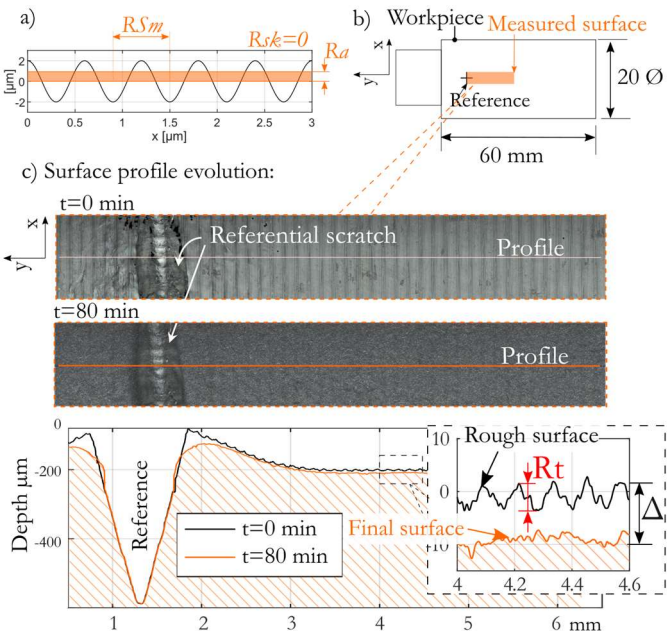

Fig.3. a) A periodical rough surface indicating *Ra, RSm* and *RSk*, b) sample geometry, and c) measurement strategy for surface profile superposition, a case where the initial topography has been totally removed.

Surface cross-section and composition

An optical microscope (ZEISS Scope.A1) has been used for imaging sample cross-sections and a scanning electron microscope SEM (TESCAN VEGA) for imaging surfaces and to analyse the composition.

Residual stresses

Residual stress measurements have been made by X-Ray diffraction method. The stress distribution in depth has been measured by gradual surface removal by electropolishing. The used parameters were: radiation Cr Kα with 20 kV, 4 mA; λ=0.229 nm, plans {211}; Bragg angle 2θ=156°; seven angles β (from -25° to +25°); oscillations β: ±3°; radiocristallographic constants: ½ S2=5.92x10-6/ MPa and S1= -1.28x10-6/ MPa.

3. Experimental program

3.1. Lubrication condition

The aim of this work is to investigate the effects of lubrication in tribofinishing processes. For this purpose, various samples have been subjected to tribofinishing varying lubrication condition:

- 5 l of liquid compound have been added to the media to humidify them before starting the polishing.
- 5 l/min of liquid compound circulated during the process. The liquid has been evacuated and filtered to eliminate the debris before resending it to the tribofinishing machine.

The test with both conditions have been repeated 2 times to prove the repeatability. In this study other parameters have been maintained constant. As explained in section 2, the sample is

dragged through the media in a circular path, so that frontal surface suffers the normal flow of media. Only the frontal surface modifications have been studied.

The executed experimental tests have been resumed in Table 2. Only lubrication rate has been varied: S-1 and S-3 have been polished with the first lubrication condition (5 l of liquid compound to humidify the media). Whereas in S-2 and S-4, the liquid compound circulated in a rate of 5 l/min and filtered to eliminate the debris before redirecting the liquid to the polishing machine.

3.2. Constant process parameters

Concerning tribofinishing parameters, spherical media composed by alumina (Al_2O_3) abrasive grains and ceramic bonder has been used. 175 kg of media of Ø 5 mm has been considered (Ref: MGA-BALL-5mm, ABC SwissTech). As far as liquid compound is concerned, a lubricant (Ref: Pulibrill 6140, ABC SwissTech), an alkaline product with a pH=8, has been dissolved with water in the respective proportions: %5 and %95. The workpiece has been dragged through media in v=1 m/s, which has determined the impact velocity of media on the frontal zone of 1 m/s.

Table 2. Experimental plan.

Sample	Media [mm]	Liquid compound
S-1	5 Ø	5 [l] (H2O + Pulib6140 %5)
S-2	5 Ø	5 [l/min] (H2O + Pulib6140 %5)
S-3	5 Ø	5 [l] (H2O + Pulib6140 %5)
S-4	5 Ø	5 [l/min] (H2O + Pulib6140 %5)

4. Results and discussion

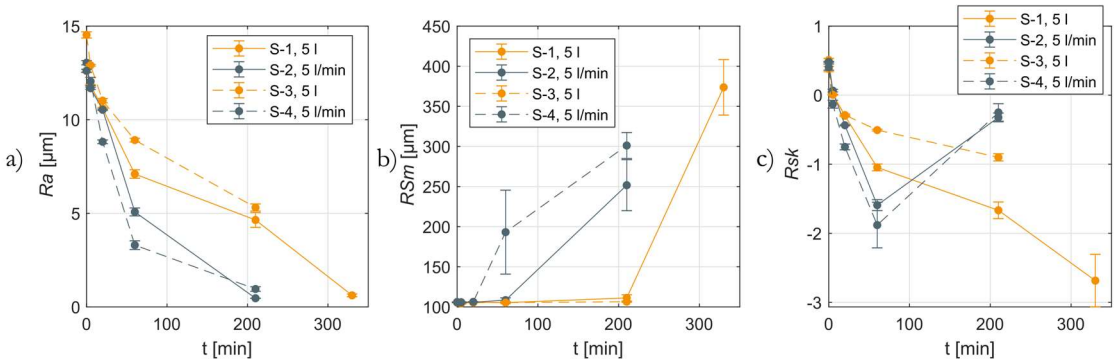

Fig.4. *Ra*, *RSm* and *Rsk* evolution.

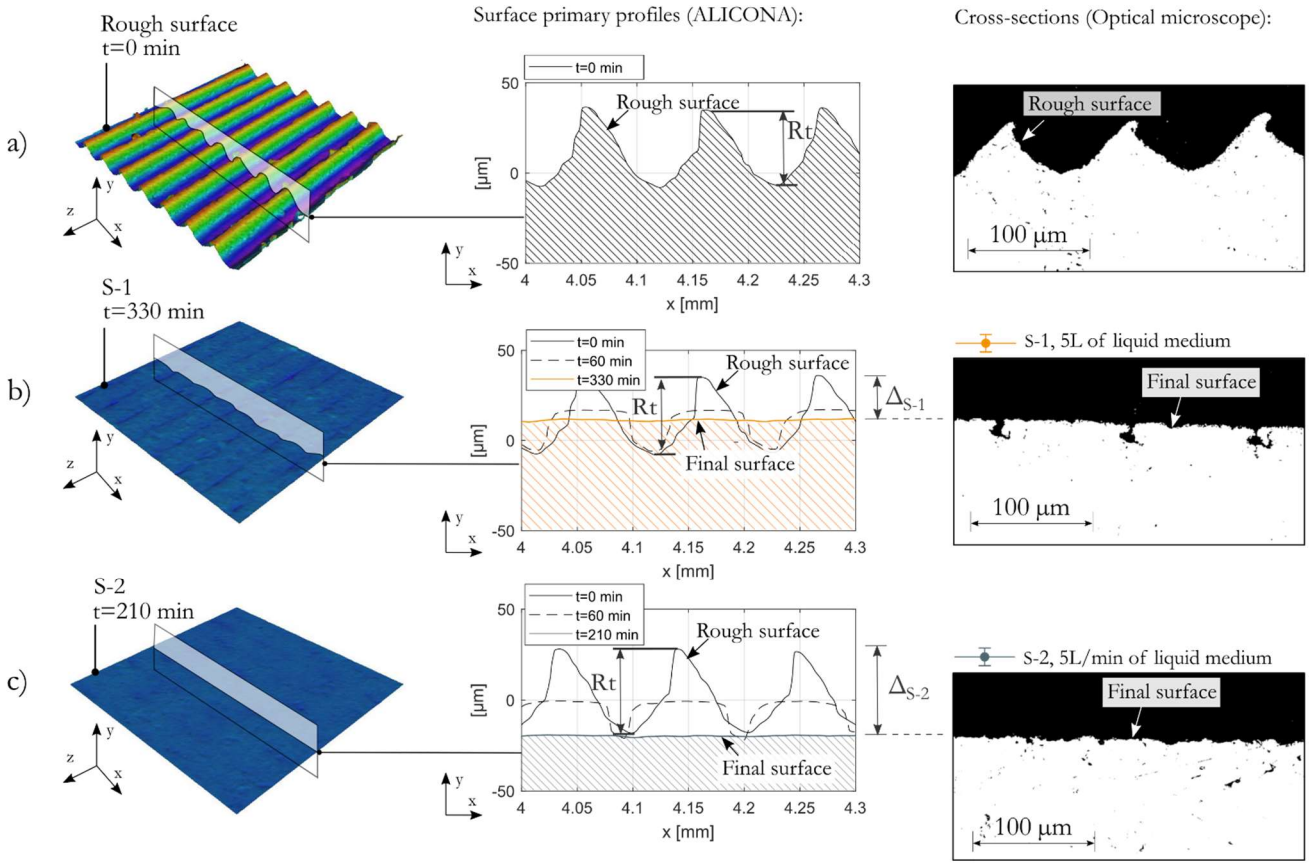

Fig.5.Surface images, profile evolutions and cross-sections for S-1 and S-2.

4.1. Surface roughness

Fig.4 shows roughness parameters evolution during process time. S-1 and S-3 (in orange color) were treated with the same conditions, without liquid compound circulation (5 l). Whereas during the test S-2 and S-4 (in gray color), the liquid compound circulation (5 l/min) has been implemented to evacuate the debris created during the process.

Ra tends to decrease with media action, whereas *RSm* increases due to the removal of the initial surface texture. Concerning *RSk*, it is directly linked to the surface plastic deformation. In general, this parameter tends to become negative with media impacts.

Fig.4 (a) shows that *Ra* evolution in S-1 and S-3 is similar. After t=120 min the value of *Ra* seems to be saturated, which is not the case for S-2 and S-4, where *Ra* reaches the value of ≈ 1 µm. Similar differences can be appreciated in Fig.4. (b) and (c). *RSm* is constant all along the process in S-1 and S-3, which means that the initial roughness profile has not been completely removed. However, S-2 and S-4 initial surface texture is removed in 210 min, as the high increase of *RSm* shows. As far as *Rsk* is concerned (Fig.4, (c)), the inflexion point at t=120 min in S-2 shows the creation of a new surface, which means that the initial surface roughness has been removed. S-1 and S-2 have been chosen for a deeper analysis. Fig.5 shows surface images, surface profiles and surface cross-sections for S-1 and S-2.

If only ALICONA surface images are observed (Fig.5), S-1 and S-2 are very similar. However, their respective surface profile offsets show how the material removal and deformation quantity is different.

Fig.5,(b) shows the surface texture, surface profiles and the cross section of S-1. The offset is $\Delta_{S\text{-}1} < R_t$, which means that initial surface texture has not been removed.

In S-2 (Fig.5, (c)), the offset $\Delta_{S\text{-}2}$ is greater than R_t ($\Delta_{S\text{-}2} > R_t$). This means the initial texture has been removed.

Surface cross-section shows how in S-1 high plastic deformation and the presence of debris is leading to a "flat" surface with cavities. Whereas in S-2, a flat surface without cavities is obtained in less process time (t=210 min).

4.2. Surface defects

SEM image in Fig. 6,(a) shows debris incrustations in the surface in sample S-1 at t=330 min due to the rests of media and workpiece material, which are stocked in the valleys. Peaks have been deformed retaining the debris in the valleys (Fig. 6,(a)).

Debris main elements are Al and Si (Fig. 6,(b).), both presents in the composition of the used abrasive media.

Regarding S-2 analysis, no debris were observed due to lubricant circulation and its filtration.

4.3. Residual stresses

This final section compares the initial stress state to the samples S-1 and S-2 after tribofinishing process. Figure 9 plots the 3 different profiles for axial and circumferential directions. At the extreme surface, compressive residual stresses (~350 MPa) have been induced after tribofinishing (Fig. 7) in both a) axial and b) circumferential axes.

In the axial direction, both profiles are similar regarding the residual stress gradients but also the affected depth (~ 100 µm).

In the circumferential direction (media flow direction), even if similar compressive stresses have been measured in the extreme surface (from 0-25 µm), the affected depth is different: ~ 25 µm for S-1 and ~ 100 µm for S-2.

This could be related to the media flow around the part in each case:

- In S-1, the reduced lubrication increases friction coefficient, reducing media flow and media tangential motion after the impact.
- In S-2, the high lubrication rate reduces friction coefficient, which results in higher media flow and tangential motion.

The tangential motion may be the responsible of greater affected depth.

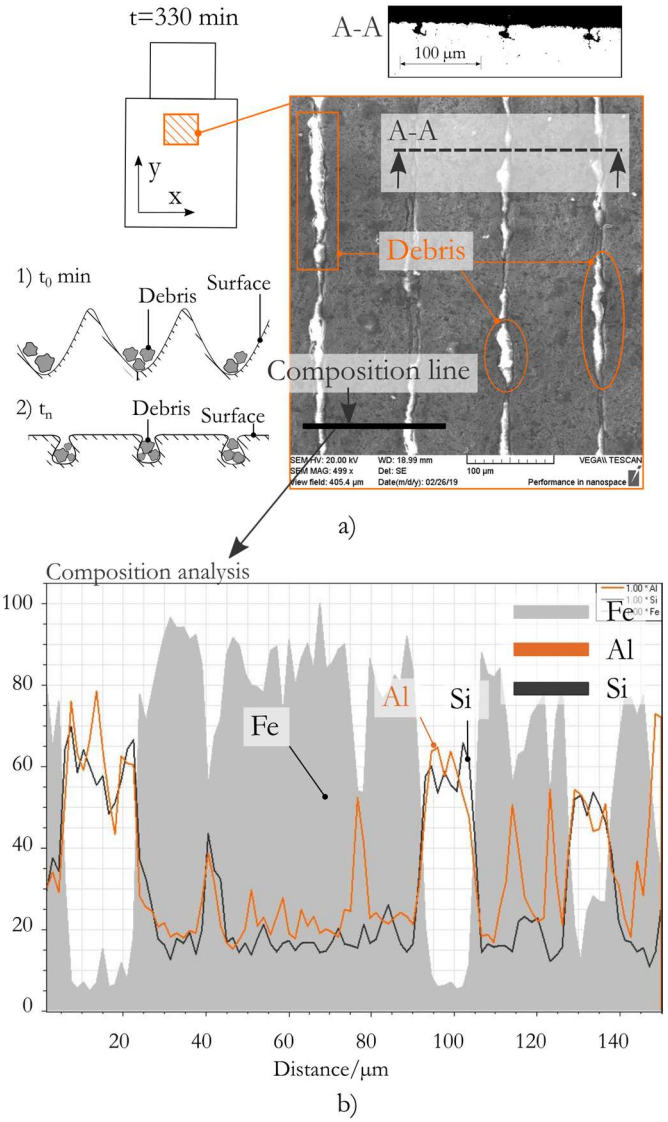

Fig. 6.a) MEB image of S-1 and schematical explanation of surface evolution, b) composition through a line in the surface of S-1.

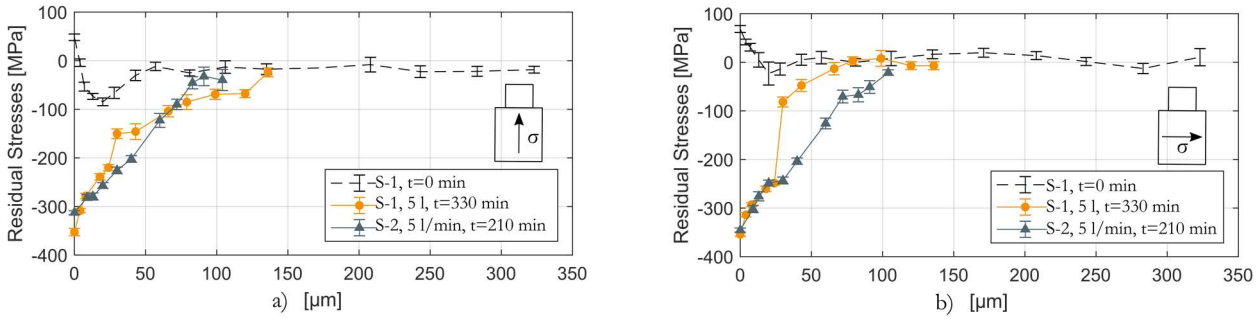

Fig. 7. Residual stress profiles in S-1 and S-2, in a) axial direction and b) circumferential direction.

5. Conclusions

This article investigated the influence of lubrication condition on the surface integrity of a drag finished part. The general conclusion is that drag finishing process is very sensitive to lubrication rate and debris evacuation. Lubrication rate modifies the media flow and the interaction between media and the surface. This leads to different abrasion and deformation mechanisms.

Lubrication rate changes friction between media-media and media-surface. With a high friction, the media flow is reduced and it has a low tangential motion after impacting the surface. However, with a low friction the tangential motion of media will be greater and it will deform and scratch the surface.

The evacuation of the debris (composed almost by Al and Si, elements that contains the used abrasive media) is also primordial to obtain a good surface finish. Otherwise, it will enter in roughness valleys and cavities avoiding the good quality of the polished surface.

It has been demonstrated that with the adequate input parameters, tribofinishing processes are able to polish very rough surfaces, reducing roughness from *Ra*~15 µm until *Ra*~1 µm. Furthermore, compressive residual stresses (~-350 MPa) are induced in the extreme surface. It can be considered that this polishing process can be used as post-processing for improving additive manufactured parts.

Both the experimental set-up and the analysis method used for this paper will be used for future investigations about material removal and deformation mechanisms during tribofinishing methods.

Acknowledgements

The authors would like to acknowledge IRT-M2P for the financial support. As well as AFTER ALM project partners.

H. Seux and H. Pascal from the laboratory of LTDS in ENISE are thanked for the fabrication of samples and XRD analysis.

References

[1] Hashimoto, F., Chaudhari, R. G., Melkote, S. N., 2016, Characteristics and Performance of Surfaces Created by Various Finishing Methods (Invited Paper), Procedia CIRP, 45:1–6, DOI:10.1016/J.PROCIR.2016.02.052.

[2] Yang, S., Li, W., 2018, Surface Finishing Theory and New Technology. Berlin, Heidelberg: Springer Berlin Heidelberg.

[3] Gillespie, L. K., 2007, Mass Finishing Handbook.

[4] Gillespie, L. K. (LaRoux K. ., 1999, Deburring and edge finishing handbook. Society of Manufacturing Engineers.

[5] Hashimoto, F., Yamaguchi, H., Krajnik, P., Wegener, K., Chaudhari, R., et al., 2016, Abrasive fine-finishing technology, CIRP Annals - Manufacturing Technology, 65/2:597–620, DOI:10.1016/j.cirp.2016.06.003.

[6] Yabuki, A., Baghbanan, M. R. R., Spelt, J. K. K., 2002, Contact forces and mechanisms in a vibratory finisher, Wear, 252/7–8:635–643, DOI:10.1016/S0043-1648(02)00016-9.

[7] Hashimoto, F., Johnson, S. P. S. P., 2015, Modeling of vibratory finishing machines, CIRP Annals - Manufacturing Technology, 64/1:345–348, DOI:10.1016/j.cirp.2015.04.004.

[8] Kang, Y. S. Y. S., Hashimoto, F., Johnson, S. P. S. P., Rhodes, J. P. J. P., 2017, Discrete element modeling of 3D media motion in vibratory finishing process, CIRP Annals - Manufacturing Technology, 66/1:313–316, DOI:10.1016/j.cirp.2017.04.092.

[9] Makiuchi, Y., Hashimoto, F., Beaucamp, A., 2019, Model of material removal in vibratory finishing, based on Preston's law and discrete element method, CIRP Annals, 68/1:365–368, DOI:10.1016/J.CIRP.2019.04.082.

[10] Song, X., Chaudhari, R., Hashimoto, F., 2014, Experimental Investigation of Vibratory Finishing Process, in *Volume 2: Processing*, p. V002T02A013.

[11] Ciampini, D., Papini, M., Spelt, J. K. K., 2007, Impact velocity measurement of media in a vibratory finisher, Journal of Materials Processing Technology, 183/2–3:347–357, DOI:10.1016/J.JMATPROTEC.2006.10.024.

[12] Ciampini, D., Papini, M., Spelt, J. K. K., 2008, Characterization of vibratory finishing using the Almen system, Wear, 264/7–8:671–678, DOI:10.1016/j.wear.2007.06.002.

[13] Pandiyan, V., Castagne, S., Subbiah, S., 2016, High Frequency and Amplitude Effects in Vibratory Media Finishing, Procedia Manufacturing, 5:546–557, DOI:10.1016/J.PROMFG.2016.08.045.

[14] Mediratta, R., Ahluwalia, K., Yeo, S. H. H., 2016, State-of-the-art on vibratory finishing in the aviation industry: an industrial and academic perspective, International Journal of Advanced Manufacturing Technology, 85/1–4:415–429, DOI:10.1007/s00170-015-7942-0.

[15] Archard, J. F., 1953, Contact and Rubbing of Flat Surfaces, Journal of Applied Physics, 24/8:981–988, DOI:10.1063/1.1721448.

[16] Uhlmann, E., Dethlefs, A., Eulitz, A., 2014, Investigation of Material Removal and Surface Topography Formation in Vibratory Finishing, Procedia CIRP, 14:25–30, DOI:10.1016/J.PROCIR.2014.03.048.

[17] Wang, S., Timsit, R. S., Spelt, J. K., 2000, Experimental investigation of vibratory finishing of aluminum, Wear, 243/1:147–156, DOI:10.1016/S0043-1648(00)00437-3.

[18] Saez-de-Buruaga, M., Esnaola, J. A., Aristimuno, P., Soler, D., Björk, T., et al., 2017, A Coupled Eulerian Lagrangian Model to Predict Fundamental Process Variables and Wear Rate on Ferrite-pearlite Steels, Procedia CIRP, 58:251–256, DOI:10.1016/J.PROCIR.2017.03.194.

[19] Grange, F., Rech, J., Kermouche, G., 2013, Procédé préparatoire, par grands déplacements, à la mise au point d'une gamme de polissage par tribofinition, FR3001170-A1.

[20] Salvatore, F., Grange, F., Kaminski, R., Claudin, C., Kermouche, G., et al., 2017, Experimental and Numerical Study of Media Action During Tribofinishing in the Case of SLM Titanium Parts, Procedia CIRP, 58:451–456, DOI:10.1016/J.PROCIR.2017.03.251.